A Computational Model for Batten Behavior in Micro Air Vehicles

Syeda Khadija F. Zaidi
A. James Clark School of Engineering
University of Maryland, College Park

Faculty Mentor: Dr. Padmanabhan Seshaiyer

Abstract

A recent interest in military surveillance and reconnaissance involves the development of Micro Air Vehicles capable of transporting surveillance equipment such as cameras and sensors to remote locations. Current designs for Micro Air Vehicles mostly involve fixed wings which may be rigid or flexible with rigid battens for support.Where not much is known about the aerodynamics of MAVs with flexible wings, this study aims to develop a computational model to describe the behavior of battens, the support structure of an MAV wing. This paper explores the development and solution of a beam model which incorporates an understanding of energy interactions. Another aim of this study is to produce accurate graphical representations of batten behavior, which would lead to a better understanding of MAV design. The simplified model can also be applied towards better understanding biological systems. Future developments in this study may involve a model for the entire wing structure, simulations based on physical parameters, as well as alternative models and methods for solving and graphing data.

This final report is submitted in partial fulfillment of the
National Science Foundation REU and Department of Defense ASSURE Program
George Mason University
June 1, 2009 July 31, 2009

Contents

List of Figures

1 Introduction

Recent advances in technology allow man to miniaturize surveillance and sensor equipment to sizes that weigh less than an ounce. Transport for such equipment is found in the form of Micro Air Vehicles, unmanned, remotely controlled aircrafts designed to travel at relatively low speeds. The small amount of materials required to build an MAV, along with its size and maneuverability make it useful for various applications such as:

- Military Reconnaissance and Surveillance
- Sensor Placement
- Search and Rescue
- Information Gathering

Originally designed for military reconnaissance, an MAV can be deployed to navigate confined spaces and gather information. In addition to image collecting, an MAV could be used to pick up or drop off sensors placed in discreet locations. Nonmilitary tasks can also benefit from the development of an MAV; tasks such as wildlife surveys, exterior surveillance of buildings and power lines, and climate studies can all implement MAVs.

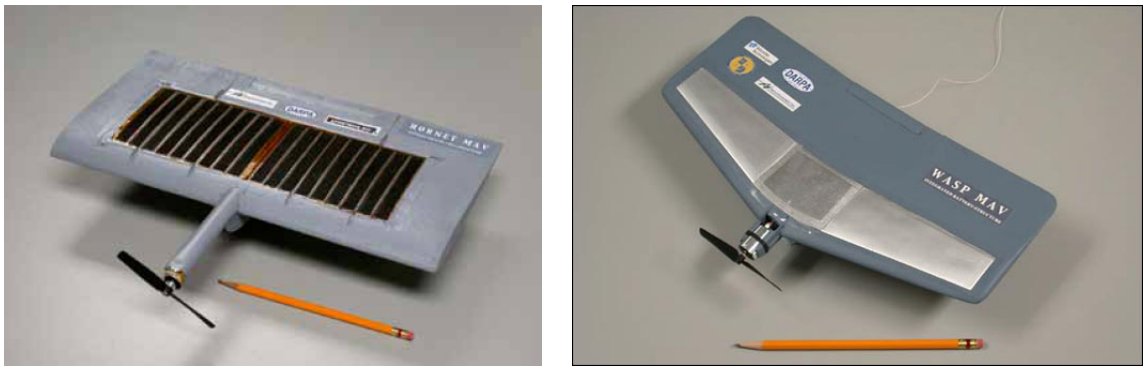

(a) The Hornet (b) The Wasp

Figure 1: Examples of Rigid-winged MAVs

While a few designs of MAVs have been produced for military use, the development of a more precise MAV with the functionality to operate for all applications mentioned above is still underway. Many early designs of MAVs focus on a rigid wing structure, such

as those displayed above. Alternatives to a rigid wing include rotating wings, motorized structures created to imitate nature, and flexible wings coupled with battens to provide some rigid support to the wing membrane.

Figure 2: Basic Micro Air Vehicle Structure

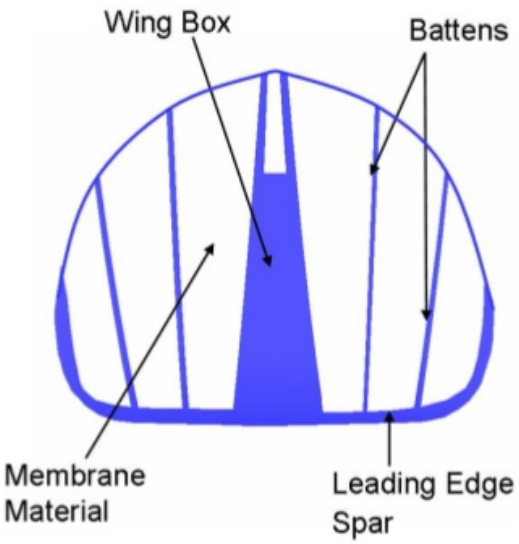

As seen above, an MAV with flexible wings has four basic elements. The wing box, which contains any equipment the MAV is designed to carry, is flanked by the wing membrane, often constructed of latex. Chord-like battens attach to a leading edge spar and the length of the wing membrane. These battens control much of the wing's movement, adding stability and flexibility to the MAV.

Figure 3: Lift Coefficients for Rigid and Flexible Winged MAVs

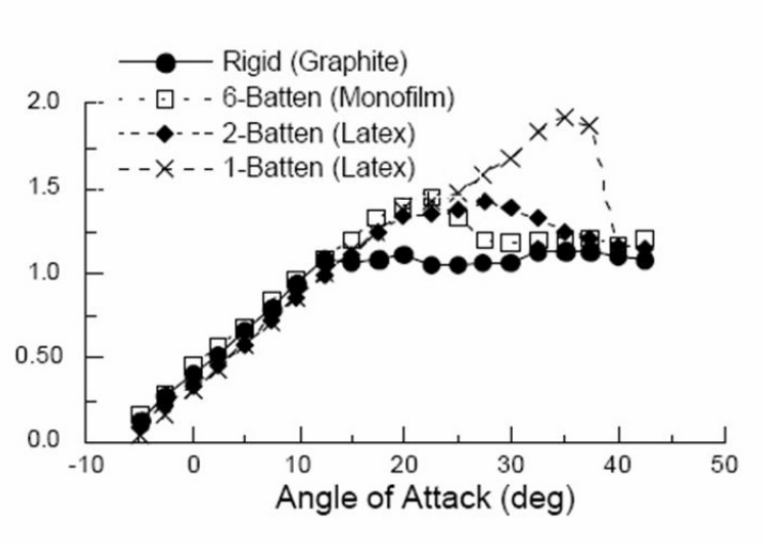

A flexible wing can provide smoother and more controlled flights, as well as a greater lift coefficient compared to a rigid fixed wing. While much is known about the aerodynamics of a rigid wing, little is known about the behavior of flexible wings. This study not only aims towards developing a model for the behavior of battens on an MAV, but also attempts to provide some insight into the behavior of flexible wings.

This paper continues with a brief background of the research methods employed in developing a model for the behavior of battens when faced with a given fluid force. After the development of a model, the paper details the methods used to solve the model, followed by a discussion of the results obtained through simulations and graphs of the mathematical model.

2 Background and Research

In developing a model for the battens of a micro air vehicle, Euler-Bernoulli beams are considered, since there is no rotation about the neutral axis (along which the beam lies). To simplify the beam model, several assumptions must be made. First, since the beam

model is based on Euler-Bernoulli beams, we assume any bending deformation occurs in one of two dimensions, omitting the neutral axis. Secondly, the beam is assumed to have a rectangular cross-section, and not a circular one. We also assume the planar cross-sections are perpendicular to the neutral axis, and that according to Kirchoff's hypothesis, these sections remain planar, rigid, and perpendicular to the neutral axis after deformation. Finally, it is assumed that the transverse displacement is significantly larger than the axial displacement. Thus the beam model developed in the following section focuses solely on the transverse displacement, ignoring the axial deformations.[1]

2.1 Development of a Beam Model

The development of a beam model can be approached in several ways. It can be developed using engineering principles or through a linear momentum approach. Both approaches focus on displacement equations describing the movement of the beam, and result in the same model.

In this paper, basic engineering principles are used to develop a model for an Euler-Bernoulli beam. This approach involves an analysis of the stress and strain experienced by the beam as it deforms. To begin, the axial and transverse deformations of the single point located on the midline of a beam are defined as

$$u_1(x, y, t) = u(x, t) - y\frac{\partial w}{\partial x}(x, t) \tag{1}$$

$$u_2(x, y, t) = w(x, t) \tag{2}$$

$$u_3(x, y, t) = 0 \tag{3}$$

where (u_1, u_2, u_3) defines the total displacement of the beam in terms of the coordinate directions (x, y, z). The axial and transverse deformations of a point on the midline of the beam are defined by $u(x, t)$ and $w(x, t)$ respectively.

Figure 4: Deformation of an Euler-Bernoulli Beam

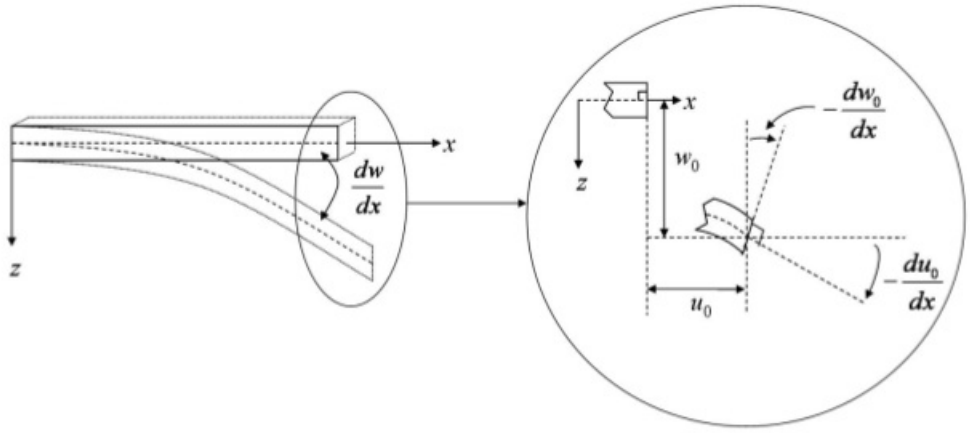

When the displacements of the beam are represented using nonlinear strain displacement relations, omitting large strain terms and preserving the term defining the rotation of a transverse normal line in the beam (the square of $\partial u_2/\partial x$) results in

$$\epsilon_{xx} = \frac{\partial u_1}{\partial x} + \frac{1}{2}(\frac{\partial u_2}{\partial x})^2 \tag{4}$$

$$\epsilon_{yy} = \frac{\partial u_2}{\partial y} \tag{5}$$

$$\epsilon_{xy} = \frac{1}{2}\left(\frac{\partial u_2}{\partial x} + \frac{\partial u_1}{\partial y}\right) \tag{6}$$

$$\epsilon_{zz} = \epsilon_{xz} = \epsilon_{yz} = 0 \tag{7}$$

Using the equations describing the displacements to define u_1 and u_2, we obtain

$$\epsilon_{xx} = \frac{\partial u}{\partial x} - y\frac{\partial^2 w}{\partial x^2} + \frac{1}{2}\left(\frac{\partial w}{\partial x}\right)^2 \tag{8}$$

$$\epsilon_{yy} = 0 \tag{9}$$

$$\epsilon_{xy} = \frac{1}{2}\left(\frac{\partial w}{\partial x} - \frac{\partial w}{\partial x}\right) = 0 \tag{10}$$

Kirchoff's stress ignoring the poisson effect is given by

$$\sigma_{xx} = E\epsilon_{xx} \tag{11}$$

2.1.1 Deriving a Non-Linear Beam Equation using Energy

The strain energy can be expressed as

$$PE_{strain} = \frac{1}{2}\int_{V_0} \sigma_{ij}\epsilon_{ij}\, dV_0 \implies \frac{1}{2}\int_{V_0} \sigma_{xx}\epsilon_{xx}\, dV_0 \implies \frac{E}{2}\int_{V_0} \epsilon_{xx}^2\, dV_0 \tag{12}$$

where V_0 is the volume of the beam before deformation, and E is the Young's Modulus. Using the expression for Kirchoff stress and the nonlinear strain displacement relations, the strain energy can be written as

$$PE_{strain} = \frac{E}{2}\int_X\int_{A_0} \left(\frac{\partial u}{\partial x} - y\frac{\partial^2 w}{\partial x^2} + \frac{1}{2}\left(\frac{\partial w}{\partial x}\right)^2\right)^2 dA_0\, dX \tag{13}$$

Expanding the integral, and then integrating over the area results in odd functions of y which disappear due to the symmetric cross-section. The moment of Inertia I_0 about the neutral axis is equal to y^2. The remaining terms are simply functions of x and t, and thus the potential energy can be written as

$$PE = \frac{1}{2}\int_0^L \left[EA_0\left(\frac{\partial u}{\partial x} + \frac{1}{2}\left(\frac{\partial w}{\partial x}\right)^2\right)^2 + EI_0\left(\frac{\partial^2 w}{\partial x^2}\right)^2\right] dX \tag{14}$$

The kinetic energy of the beam is written as

$$KE = \frac{1}{2}\int_0^L \int_{A_0} \rho\left(\left(\frac{\partial u_1}{\partial t}\right)^2 + \left(\frac{\partial u_2}{\partial t}\right)^2\right) dA_0\, dx \tag{15}$$

Using the expressions describing the displacements and omitting any terms pertaining to the axial displacement, we once again expand the integral and integrate over the area.

The symmetric cross-section causes odd functions of y to disappear, while y^2 becomes the moment of inertia I_0 about the neutral axis. The resulting expression is

$$KE = \frac{1}{2}\int_0^L \left[\rho A_0 \left(\frac{\partial u}{\partial t}^2 + \frac{\partial w}{\partial t}^2\right) + \rho I_0 \left(\frac{\partial^2 w}{\partial t \partial x}\right)^2\right] dx \tag{16}$$

The term $\rho I_0 \left(\frac{\partial^2 w}{\partial t \partial x}\right)^2$ is the Rayleigh's rotational term, which describes the kinetic energy due to the cross-section's rotation. It is assumed to be zero for our purposes.

2.1.2 Hamilton's Principle

The equations of motion and the boundary conditions describing the behavior of the beam can be achieved via Hamilton's principle. [3]

The Lagrangian integrated over time is

$$\int_{t_i}^{t_f} L\, dt = \int_{t_i}^{t_f} (KE - PE)\, dt \tag{17}$$

$$\begin{aligned}\int_{t_i}^{t_f} L\, dt \;\; = \;\; & \frac{1}{2}\int_{t_i}^{t_f}\int_0^L \left[\rho A_0 \left(\frac{\partial u}{\partial t}^2 + \frac{\partial w}{\partial t}^2\right)\right] - \\ & \left[EA_0 \left(\frac{\partial u}{\partial x} + \frac{1}{2}\left(\frac{\partial w}{\partial x}\right)^2\right)^2 + EI_0 \left(\frac{\partial^2 w}{\partial x^2}\right)^2\right] dx\, dt\end{aligned} \tag{18}$$

And the work done by the transverse and axial forces is given by

$$\delta W = \int_0^L \left(\left\{F(x,t) - K\frac{\partial w}{\partial t}\right\}\delta w + p(x,t)\delta u\right) dx \tag{19}$$

where $F(x,t)$ is the fluid force encountered by the micro air vehicle, and $K\frac{\partial w}{\partial t}$ is the damping effect of the wave. To simplify the model further, the damping effect is assumed to be zero, as is the pressure p experienced by the MAV.

The variation of (18) results in

$$\int_{ti}^{tf}\int_0^L \rho A_0 \left(\frac{\partial u}{\partial t}\delta\frac{\partial u}{\partial x} + \frac{\partial w}{\partial t}\delta\frac{\partial w}{\partial t}\right) \tag{20}$$

$$- EA_0\left(\frac{\partial u}{\partial x} + \frac{1}{2}\left(\frac{\partial w}{\partial x}\right)^2\right)\left(\delta\frac{\partial u}{\partial x} + \frac{\partial w}{\partial x}\delta\frac{\partial w}{\partial x}\right) \tag{21}$$

$$- EI_0\left(\frac{\partial^2 w}{\partial x^2}\delta\frac{\partial^2 w}{\partial x^2}\right)\,dx\,dt$$

Consider the integration by parts of this term:

$$\int_0^L \rho A_0\left(\frac{\partial w}{\partial t}\delta\frac{\partial w}{\partial t}\right)\,dx = \rho A_0\frac{\partial w}{\partial t}\delta w\Big|_0^L - \rho A_0\int_0^L \frac{\partial^2 w}{\partial t^2}\delta w \tag{22}$$

where the variation at the end points in time is assumed to be zero. Continuing to integrate each term in (20), we obtain

$$\int_{ti}^{tf}\left[\int_0^L\left\{-\rho A_0\frac{\partial^2 u}{\partial t^2} + \frac{\partial}{\partial x}\left[EA_0\left(\frac{\partial u}{\partial x} + \frac{1}{2}\left(\frac{\partial w}{\partial x}\right)^2\right)\right]\right\}\delta u \tag{23}$$

$$+\left\{-\rho A_0\frac{\partial^2 w}{\partial t^2} + \frac{\partial}{\partial x}\left(EA_0\left(\frac{\partial u}{\partial x} + \frac{1}{2}\left(\frac{\partial w}{\partial x}\right)^2\right)\frac{\partial w}{\partial x}\right) - \frac{\partial^2}{\partial x^2}\left(EI_0\frac{\partial^2 w}{\partial x^2}\right)\right\}\delta w\,dX\Bigg]\,dt$$

$$+\int_{ti}^{tf}\left\{\left[\frac{\partial}{\partial x}\left(EI_0\frac{\partial^2 w}{\partial x^2}\right) - EA_0\left(\frac{\partial u}{\partial x} + \frac{1}{2}\left(\frac{\partial w}{\partial x}\right)^2\right)\frac{\partial w}{\partial x}\right]\delta w\right\}\Big|_0^L dt$$

$$+\int_{ti}^{tf}\left\{-EA_0\left(\frac{\partial u}{\partial x} + \frac{1}{2}\left(\frac{\partial w}{\partial x}\right)^2\right)\delta u - EI_0\frac{\partial^2 w}{\partial x^2}\delta\frac{\partial w}{\partial x}\right\}\Big|_0^L dt$$

According to Hamilton's Principle, [3]

$$\delta\int_{ti}^{tf}(L - W)\,dt = 0 \tag{24}$$

(23) simplifies to the following nonlinear coupled equations

$$\rho A_0 \frac{\partial^2 u}{\partial t^2} - \frac{\partial}{\partial x}\left[EA_0\left(\frac{\partial u}{\partial x} + \frac{1}{2}\left(\frac{\partial w}{\partial x}\right)^2\right)\right] = p = 0$$

$$\rho A_0 \frac{\partial^2 w}{\partial t^2} - \frac{\partial}{\partial x}\left[EA_0\left(\frac{\partial u}{\partial x} + \frac{1}{2}\left(\frac{\partial w}{\partial x}\right)^2\right)\frac{\partial w}{\partial x}\right] + EI_0\frac{\partial^4 w}{\partial x^4} = F(x,t) \tag{25}$$

with boundary conditions

$$EA_0\left(\frac{\partial u}{\partial x} + \frac{1}{2}\left(\frac{\partial w}{\partial x}\right)^2\right)\delta u\Big|_0^L = 0$$

$$\left[\frac{\partial}{\partial x}\left(EI_0\frac{\partial^2 w}{\partial x^2}\right) - EA_0\left(\frac{\partial u}{\partial x} + \frac{1}{2}\left(\frac{\partial w}{\partial x}\right)^2\right)\right]\delta w\Big|_0^L = 0 \tag{26}$$

$$EI_0\frac{\partial^2 w}{\partial x^2}\delta\frac{\partial w}{\partial x}(L,t) = 0$$

Non-dimensionalizing each term would result in a model based solely on the transverse deformations of the beam; however, retaining all dimensions allows the code to be customized to different properties of a batten, such as the Young's Modulus or the cross-sectional area of the beam. To simplify the model further while solving, the Young's Modulus E, the cross-sectional area A_0, the density ρ, and the moment of Inertia I_0 are all taken to equal 1.

One term remains to be simplified; $\left(\frac{\partial u}{\partial x} + \frac{1}{2}\left(\frac{\partial w}{\partial x}\right)^2\right)$ is assumed to be a function of t only; i.e. h(t)=$\left(\frac{\partial u}{\partial x} + \frac{1}{2}\left(\frac{\partial w}{\partial x}\right)^2\right)$. We also assume the following boundary conditions:

$$u(0,t) = 0$$

$$u(L,t) = 0$$

Taking the definite integral of this term with respect to x, we obtain

$$\int_0^1 h(t)\,dx = \int_0^1 \left[\frac{\partial u}{\partial x} + \frac{1}{2}\left(\frac{\partial w}{\partial x}\right)^2\right] dx$$

$$xh(t)\Big|_0^1 = u(x,t)\Big|_0^1 + \frac{1}{2}\int_0^1 \left(\frac{\partial w}{\partial x}\right)^2 dx$$

$$h(t) = \frac{1}{2}\int_0^1 \left(\frac{\partial w}{\partial x}\right)^2 dx \tag{27}$$

Substituting this back into the expression simplifies to the following beam model

$$\frac{\partial^4 u}{\partial^4 x} + \frac{\partial^2 u}{\partial^2 t} - \frac{1}{2}\frac{\partial^2 u}{\partial^2 x}\int_0^L \left(\frac{\partial u}{\partial x}\right)^2 = F(x,t) \tag{28}$$

2.2 Solving the Beam Model

In this section, the beam model is solved using the Finite Differences method; by approximating each differential term through the center differences method, a scheme can be written to solve the model over multiple iterations. The model is solved explicitly in this paper; it is also possible to compute an implicit scheme for the beam model.

The model:

$$\frac{\partial^4 u}{\partial^4 x} + \frac{\partial^2 u}{\partial^2 t} - \frac{1}{2}\frac{\partial^2 u}{\partial^2 x}\int_0^L \left(\frac{\partial u}{\partial x}\right)^2 = F(x,t)$$

Initial Conditions: $u(x,0) = f(x)$ $u_t(x,0) = g(x)$

where the beam is taken to be a length L. In the previous section, the variable u was used to represent the axial displacement; in this section, the variable u is taken to represent the transverse displacement instead of the variable w.

Rewriting each term by replacing it with the center differences approximation results

in

$$\frac{u_i^{n+1} - 2u_i^n + u_i^{n-1}}{\triangle t^2} + \frac{u_{i-2}^n - 4u_{i-1}^n + 6u_i^n - 4u_{i+1}^n + u_{i+2}^n}{\triangle x^4} - \frac{1}{2} I \frac{u_{i-1}^n - 2u_i^n + u_{i+1}^n}{\triangle x^2} = F(x,t) \tag{29}$$

where $F(x,t)$ is the external fluid force and I signifies the integral which is part of the nonlinear term. We will later see that this value is simply a number computed during iterations of the overall model.

Solving for u_i^{n+1}, (29) becomes

$$\begin{aligned} u_i^{n+1} &= \frac{\triangle t^2}{\triangle x^4}\left(-u_{i-2}^n + 4u_{i-1}^n - 6u_i^n + 4u_{i+1}^n - u_{i+2}^n\right) - \\ &\quad \frac{1}{2} I \triangle t^2 \left(u_{i-1}^n - 2u_i^n + u_{i+1}^n\right) + 2u_i^n - u_i^{n-1} + F(x,t)\triangle t^2 \end{aligned} \tag{30}$$

Beyond this point, $\frac{\triangle t^2}{\triangle x^4}$ is referred to as λ. Taking n=0 and repeating the model for different values of i illustrates the scheme. For example

$$\begin{aligned} u_1^1 &= \lambda\left(-u_{-1}^0 + 4u_0^0 - 6u_1^0 + 4u_2^0 - u_3^0\right) - \\ &\quad \frac{1}{2}\triangle t^2 \left(u_0^0 - 2u_1^0 + u_2^0\right) + 2u_1^0 - u_1^{-1} + F(x,t)\triangle t^2 \end{aligned}$$

$$\begin{aligned} u_2^1 &= \lambda\left(-u_0^0 + 4u_1^0 - 6u_2^0 + 4u_3^0 - u_4^0\right) - \\ &\quad \frac{1}{2}\triangle t^2 \left(u_1^0 - 2u_2^0 + u_3^0\right) + 2u_2^0 - u_2^{-1} + F(x,t)\triangle t^2 \end{aligned}$$

$$\cdots$$

$$\cdots$$

$$u^1_{M-2} = \lambda\left(-u^0_{M-4} + 4u^0_{M-3} - 6u^0_{M-2} + 4u^0_{M-1} - u^0_M\right) - \frac{1}{2}\triangle t^2\left(u^0_{M-3} - 2u^0_{M-2} + u^0_{M-1}\right) + 2u^0_{M-2} - u^{-1}_{M-2} + F(x,t)\triangle t^2$$

$$u^1_{M-1} = \lambda\left(-u^0_{M-3} + 4u^0_{M-2} - 6u^0_{M-1} + 4u^0_M - u^0_{M+1}\right) - \frac{1}{2}\triangle t^2\left(u^0_{M-2} - 2u^0_{M-1} + u^0_M\right) + 2u^0_{M-1} - u^{-1}_{M-1} + F(x,t)\triangle t^2$$

This results in M-1 equations, where M signifies the right boundary point.

Some values in the scheme can be determined through the boundary conditions. The boundary conditions for a beam which is clamped at both ends[4] (the initial assumption for the beam's boundary in this paper) are known to be

$$u(0,t) = 0 \tag{31}$$

$$u(L,t) = 0$$

$$u_x(0,t) = 0 \tag{32}$$

$$u_x(L,t) = 0$$

For example, the first boundary conditions show u^0_0 to be zero, since the beam is clamped at that end. The same is true for the right boundary point M; u^0_M is equal to zero.

Consider the first of the second set of boundary conditions:

$$u_x(0,t) = 0$$

Rewriting this boundary condition using a center approximation results in:

$$\frac{u(\triangle x, t) - u(-\triangle x, t)}{2 \triangle x} = 0$$

$$u(\triangle x, t_n) = u(-\triangle x, t_n)$$

Therefore, at n=0

$$u_1^0 = u_{-1}^0$$

The same method is used to utilize the second of the set of boundary conditions:

$$u_x(L, t) = 0$$

$$\frac{u(L + \triangle x, t) - u(L - \triangle x, t)}{2 \triangle x} = 0$$

$$u(L + \triangle x, t_n) = u(L - \triangle x, t_n)$$

$$\therefore u_{M+1}^0 = u_{M-1}^0$$

Once a few iterations of the model are written out, a clear scheme can be written to express the solution

$$\begin{bmatrix} u_1^1 \\ u_2^1 \\ \cdots \\ u_{M-2}^1 \\ u_{M-1}^1 \end{bmatrix} = \begin{bmatrix} a & b & c & & \\ b & d & b & c & \\ c & b & d & b & c \\ & c & b & d & b \\ & & c & b & a \end{bmatrix} \begin{bmatrix} u_1^0 \\ u_2^0 \\ \cdots \\ u_{M-2}^0 \\ u_{M-1}^0 \end{bmatrix} - \begin{bmatrix} u_1^- 1 \\ u_2^- 1 \\ \cdots \\ u_{M-2}^- 1 \\ u_{M-1}^- 1 \end{bmatrix} + F(x,t) \triangle t^2 \qquad (33)$$

where

$$a = 2 - 7r - rI \triangle x^2$$
$$b = 4r + \frac{1}{2} rI \triangle x^2$$
$$c = -r$$
$$d = 2 - 6r - rI \triangle x^2$$

Which can be summarized

$$U^{(n+1)} = AU^{(n)} - U^{(n-1)} + F(x,t) \triangle t^2 \tag{34}$$

The initial conditions must now be used to compute $\vec{U^{(0)}}$ in the first iteration of the scheme.

$$u(x,0) = f(x)$$
$$u(x_j,0) = f(x_j)$$
$$\therefore u_1^0 = f(1)$$
$$u_2^0 = f(2)$$
$$\dots$$
$$u_M - 2^0 = f(M-2)$$
$$u_M - 1^0 = f(M-1)$$
$$\therefore \vec{U^{(0)}} = \vec{f}$$

The first iteration in time for the scheme also has the term $\vec{U^{(-1)}}$ which can also be

taken care of using the initial conditions

$$u_t(x,0) = g(x)$$

$$\frac{u(x,\triangle t) - u(x,-\triangle t)}{2\triangle t} = g(x)$$

$$u(x,\triangle t) - u(x,-\triangle t) = 2\triangle t\, g(x)$$

$$u_1^1 - u_1^{-1} = 2\triangle t\, g_1$$

$$u_2^1 - u_2^{-1} = 2\triangle t\, g_2$$

$$\cdots$$

$$u_{M-2}^1 - u_{M-2}^{-1} = 2\triangle t\, g_{M-2}$$

$$u_{M-1}^1 - u_{M-1}^{-1} = 2\triangle t\, g_{M-1}$$

$$\therefore \vec{U^{(1)}} - \vec{U^{(-1)}} = 2\triangle t\, \vec{g} \qquad\qquad \therefore \vec{U^{(-1)}} = \vec{U^{(1)}} - 2\triangle t\, \vec{g}$$

Therefore, for the first iteration, the scheme must be taken as

$$U^{(1)} = \frac{1}{2}A\vec{f} + \triangle t\vec{g} + \frac{1}{2}F(x,t)\triangle t^2 \tag{35}$$

The complete scheme for solving the Beam Model is therefore:

$$U^{(1)} = \frac{1}{2}A\vec{f} + \triangle t\vec{g} + \frac{1}{2}F(x,t)\triangle t^2$$

$$U^{(n+1)} = AU^{(n)} - U^{(n-1)} + F(x,t)\triangle t^2 \tag{36}$$

2.3 Coding for a Solution

A solution for the explicit scheme developed earlier in this section can be graphed using MATLAB. The scheme can be iterated a number of times employing a loop, producing multiple graphs depicting batten behavior.

The code is structured as follows

Primary Iteration of scheme with a given fluid force

$\downarrow$

Output of $\vec{U^{(n)}}$

$\downarrow$

Computation of I (Integral value) using input $\vec{U^{(n)}}$ and trapezoidal rule

$\downarrow$

Update the value of I within scheme

$\downarrow$

Further Iterations of scheme, repeating procedure of updating I

$\downarrow$

Established tolerance $\epsilon \leq |u_{new} - u_{old}|$ causes iterations to cease

$\downarrow$

Plot produced of final output of the transverse displacement

3 Results and Discussion

The output of the code described in the preceding section is represented as a set of curves which appear bound at either end.

Figure 5: Clamped Clamped Beam

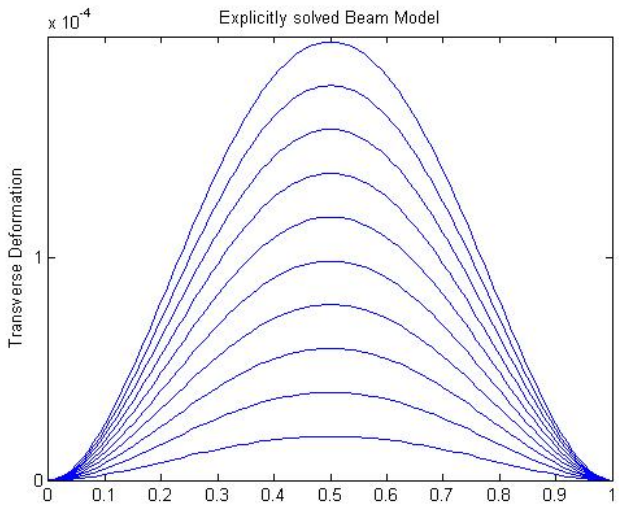

The set of boundary conditions used to interpret the scheme describe the behavior of a beam which is clamped at both ends.[4] While this is useful in understanding the code and testing the accuracy of the algorithm, the actual conditions that must be used to represent a batten should describe the behavior of a cantilever beam; i.e. one that is clamped at one end and free at the other[2]. The difficulty in producing a representation for a cantilever beam lies in describing the boundary conditions. An exact solution for such a system has very specific conditions; namely, while the second and third derivative must equal zero, the first must not. Future work in this study would primarily focus on finding an appropriate solution for a cantilever beam, so that the code may be designed to hold true for the exact solution found.

Attempting to produce graphs for a cantilever using an exact solution similar to one that can be used to describe a clamped clamped beam resulted in a graph which continued

to appear clamped at the right end, despite the slight difference in behavior.

Figure 6: An Attempt to Graphically represent a Cantilever Beam

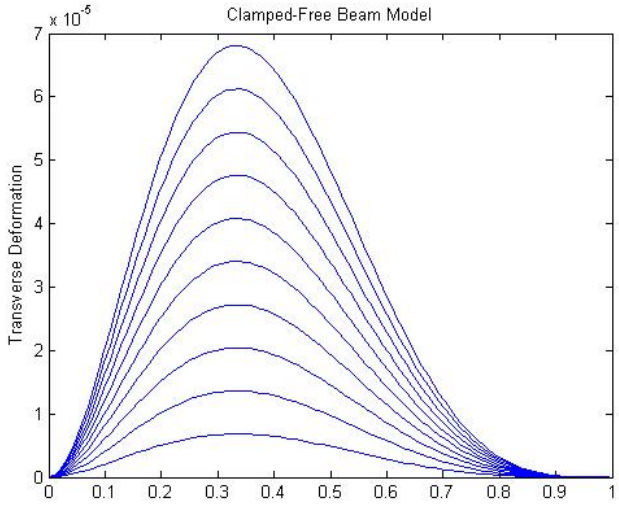

The significance of these graphs is that they provide a prediction for the behavior of micro air vehicles designed with flexible wings. However, these graphs cannot be interpreted alone. A model for the one-dimensional wing must be developed and coupled with the batten model to produce graphs which hold valuable information about the aerodynamics of a flexible wing.

Alternative batten layouts for MAVs must also be studied as a result of this study; for example, battens could be constructed to be clamped, free, pinned, or even sliding at either edge, allowing for a variety of designs to be considered and understood.

Also as a result of this study, alternative models must be computed in a similar procedure to allow for comparison to better judge the accuracy of such a model. These alternative models should be studied alongside experimental data and simulations, so that a more complete model can be developed and tested against information that is known.

4 Conclusion

This study barely skims the surface of all that is possible with a thorough understanding of batten behavior for MAVs. Not only would an understanding lead to advancements in design, but there would also be the possibility of applying the understanding to biological systems. An understanding of nature would feed back to the study of MAV and a fully functional design.

There remains much opportunity for future work. Beside coupling the beam model with a wing model, it is also necessary to model the MAV as a whole and understand every aspect of flight behavior. The approach discussed in this paper can be applied to other computational modeling studies as well, to develop newer models which could produce representations of entire MAVs.

Alternative wings could also be modeled as a way of generating data to constantly compare research against. Not only would alternative wings produce more models, but also more options would be made available to those physically designing functional MAVs.

This study involved using simple methods which could also be employed in a classroom setting to allow for a better understanding of other subjects in mathematics and physics. The implications of this study are not solely in the field of science and research, but in the field of education as well. This paper can only cover a small percentage of the significance of this study.

References

[1] Lauren A. Ferguson, *A Computational Model for Flexible Wing Based Micro Air Vehicles*, 2006.

[2] Morgul,O, *Dynamic Boundary Control of an Euler-Bernoulli Beam*, IEEE, 1992.

[3] Rick Salmon, *Practical Use of Hamilton's principle*, Journal of Fluid Mechanics, 2006.

[4] Tony L. Schmitz, Kevin S. Smith, *Machining Dynamics*, Springer, 2008.